UCRL-16681-Rev.

University of California

Ernest O. Lawrence Radiation Laboratory

DIFFUSIONAL EFFECTS IN THE GERMANIUM-IODINE REACTION

TWO-WEEK LOAN COPY

This is a Library Circulating Copy
which may be borrowed for two weeks.
For a personal retention copy, call
Tech. Info. Division, Ext. 5545

Berkeley, California

DISCLAIMER

This document was prepared as an account of work sponsored by the United States Government. While this document is believed to contain correct information, neither the United States Government nor any agency thereof, nor the Regents of the University of California, nor any of their employees, makes any warranty, express or implied, or assumes any legal responsibility for the accuracy, completeness, or usefulness of any information, apparatus, product, or process disclosed, or represents that its use would not infringe privately owned rights. Reference herein to any specific commercial product, process, or service by its trade name, trademark, manufacturer, or otherwise, does not necessarily constitute or imply its endorsement, recommendation, or favoring by the United States Government or any agency thereof, or the Regents of the University of California. The views and opinions of authors expressed herein do not necessarily state or reflect those of the United States Government or any agency thereof or the Regents of the University of California.

Submitted to A. I. Ch. E. J.

UCRL-16681 Rev.

UNIVERSITY OF CALIFORNIA

Lawrence Radiation Laboratory
Berkeley, California

AEC Contract No. W-7405-eng-48

DIFFUSIONAL EFFECTS IN THE GERMANIUM-IODINE REACTION

Donald R. Olander

(October 1966)

DIFFUSIONAL EFFECTS IN THE GERMANIUM-IODINE REACTION

Donald R. Olander

Inorganic Materials Research Division,
Lawrence Radiation Laboratory
and the Department of Nuclear Engineering,
University of California, Berkeley, California

October 1966

ABSTRACT

The momentum, overall continuity and two diffusion equations governing rotating disk mass transfer in a ternary system with a reaction boundary condition have been derived. The effects of variable density, interfacial velocity, and multicomponent diffusion have been considered. The theory has been compared to experimental data obtained for the I_2-GeI_4-diluent system. Absolute prediction of the transfer rate in the dilute I_2-GeI_4 region was within 15% of the experimental results. In the concentrated reactant gas region, the conservation equations were solved by an approximate method which permitted the effects of density variation in the flow equations, interfacial velocity, and density variations and multicomponent effects in the diffusion equations to be evaluated independently. Theory and experiment were compared by examining the variation of the ratio of the mass transfer coefficients in the concentrated and dilute reactant gas regions as a function of iodine concentration. For iodine mole fractions between zero and unity and helium and argon diluents, the theory was consistently 7-10% below the experimental data.

INTRODUCTION

In the previous paper, those aspects of the germanium-iodine reaction dominated by surface kinetics were examined. In this study, the diffusion limited region will be considered in detail.

The measured rates will be compared with theoretical predictions based on solution of the conservation equations. The combined effects of density variations in the boundary layer, multicomponent diffusion, and interfacial velocities on the rate will be demonstrated theoretically and experimentally.

All experiments were conducted at 415°C, in the region of complete diffusion control. Since the reaction between gaseous iodine and solid germanium is essentially irreversible, the concentration of iodine at the germanium disk surface is zero in all cases. The sole product of the reaction is gaseous GeI_4. The system is assumed isothermal and viscosity variations through the boundary layer are neglected. Neither of these simplifications are entirely valid: The bulk gas phase was ~20°C hotter than the disk surface, and the change in composition from iodine-diluent in the bulk to GeI_4-diluent at the disk surface is probably accompanied by an increase in viscosity. However, because the disk surface was cooler than the bulk gas, the composition-induced viscosity increase is at least partially nullified by a temperature effect in the opposite direction.

Similarly, natural convection effects superimposed upon the forced flow because of the unstable temperature profile have been neglected in the theoretical development. The range of validity of this assumption will be assessed when theory and experiment are compared.

Conservation Equations

The momentum equations governing the flow about a rotating disk are those appropriate to an axisymmetric, cylindrical geometry. For compressible flow, these are:

radial component:

$$\rho\left[u\frac{\partial u}{\partial r} + w\frac{\partial u}{\partial z} - \frac{v^2}{r}\right] = \mu\left[\frac{\partial^2 u}{\partial r^2} + \frac{\partial}{\partial r}\left(\frac{u}{r}\right) + \frac{\partial^2 u}{\partial z^2} + \frac{1}{3}\frac{\partial}{\partial r}(\nabla\cdot v)\right] \qquad (1)$$

where

$$\nabla \cdot v = \frac{1}{r}\frac{\partial}{\partial r}(ru) + \frac{\partial w}{\partial z} \qquad (2)$$

For the rotating disk system, the radial pressure gradient is zero.

angular component:

$$\rho\left[u\frac{\partial v}{\partial r} + w\frac{\partial v}{\partial z} + \frac{uv}{r}\right] = \mu\left[\frac{\partial^2 v}{\partial r^2} + \frac{\partial}{\partial r}\left(\frac{v}{r}\right) + \frac{\partial^2 v}{\partial z^2}\right] \qquad (3)$$

In Eqs. (1) and (3), the viscosity of the gas is assumed constant at the bulk value. The overall continuity equation is:

$$\frac{1}{r}\frac{\partial}{\partial r}(\rho r u) + \frac{\partial}{\partial z}(\rho w) = 0 \qquad (4)$$

Since the system contains three components, two species conservation equations are required:

$$\rho \underline{v} \cdot \nabla \omega_i = -\nabla \cdot \underline{j}_i \qquad (i = 1,2) \qquad (5)$$

The relation between the $\underline{j}_i$ and the multicomponent diffusion coefficients can be written as:[2]

$$\underline{j}_i = \frac{C^2}{\rho} \sum_{k=1}^{3} M_i M_k D_{ik} \nabla x_k \tag{6}$$

The multicomponent diffusion coefficients are related to the binary diffusion coefficients by virtue of the Maxwell-Stephan relations:

$$D_{ii} = 0 \tag{7a}$$

$$D_{12} = \mathcal{D}_{12} \left[1 + x_3 (\mathcal{D}_{13} M_3 / M_2 - \mathcal{D}_{12}) / \bar{\mathcal{D}} \right] \tag{7b}$$

$$D_{13} = \mathcal{D}_{13} \left[1 + x_2 (\mathcal{D}_{12} M_2 / M_3 - \mathcal{D}_{13}) / \bar{\mathcal{D}} \right] \tag{7c}$$

$$D_{21} = \mathcal{D}_{12} \left[1 + x_3 (\mathcal{D}_{23} M_3 / M_1 - \mathcal{D}_{12}) / \bar{\mathcal{D}} \right] \tag{7d}$$

$$D_{23} = \mathcal{D}_{23} \left[1 + x_1 (\mathcal{D}_{12} M_1 / M_3 - \mathcal{D}_{23}) / \bar{\mathcal{D}} \right] \tag{7e}$$

$$\bar{\mathcal{D}} = x_1 \mathcal{D}_{23} + x_2 \mathcal{D}_{13} + x_3 \mathcal{D}_{12} \tag{7f}$$

Mole and mass fraction are related by

$$\omega_i = M_i x_i / \bar{M} \tag{8}$$

where

$$\bar{M} = x_1 M_1 + x_2 M_2 + x_3 M_3 \tag{9}$$

In an isothermal, ideal gas system, the total concentration, C, is constant and

$$\rho = \bar{M} C \tag{10}$$

<u>Dimensionless Equations</u>

Before setting out the boundary conditions, the conservation equation

will be non-dimensionalized. Since on a rotating disk, the concentration varies with axial position only, $\rho = \rho(z)$ and $x_i = x_i(z)$. The velocity components are non-dimensionalized by:

$$u = r\Omega F(\xi) \tag{11}$$

$$v = r\Omega G(\xi) \tag{12}$$

$$w = \sqrt{\nu_\infty \Omega}\, H(\xi) \tag{13}$$

where

$$\nu_\infty = \mu/\rho_\infty \tag{14}$$

and

$$\xi = (\Omega/\nu_\infty)^{1/2} z \tag{15}$$

with these transformations, Eqs. (1), (3), and (4) become:

$$(\rho/\rho_\infty)(F^2 - G^2) + \left(\frac{\rho}{\rho_\infty} H\right) F' = F'' \tag{16}$$

$$2(\rho/\rho_\infty)FG + \left(\frac{\rho}{\rho_\infty} H\right) G' = G'' \tag{17}$$

$$2(\rho/\rho_\infty)F + \left(\frac{\rho}{\rho_\infty} H\right)' = 0 \tag{18}$$

Except for the density ratio sprinkled throughout, these relations are those given by Schlichting.[7]

Converting the mass fractions on the left of Eq. (5) to mole fractions by Eq. (8), the diffusion equations become:

$$\frac{N_{Sc_{13}} H(\xi)}{\rho/\rho_\infty} \left(a_1 \frac{dx_1}{d\xi} + a_2 \frac{dx_2}{d\xi}\right) = \frac{d}{d\xi}\left[\frac{1}{\rho/\rho_\infty}\left(b_1 \frac{dx_1}{d\xi} + b_2 \frac{dx_2}{d\xi}\right)\right] \tag{19}$$

$$\frac{N_{Sc_{13}} H(\xi)}{\rho/\rho_\infty} \left(c_1 \frac{dx_1}{d\xi} + c_2 \frac{dx_2}{d\xi}\right) = \frac{d}{d\xi}\left[\frac{1}{\rho/\rho_\infty}\left(e_1 \frac{dx_1}{d\xi} + e_2 \frac{dx_2}{d\xi}\right)\right] \tag{20}$$

where

$$a_1 = (S_2 - 1)x_2 + 1 \tag{21}$$

$$a_2 = -(S_2 - 1)x_1 \tag{22}$$

$$b_1 = \frac{1 + (R_2 - 1)x_1 + (S_2 - 1)x_2}{1 + (R_2 - 1)x_1 + (R_1 - 1)x_2} \tag{23}$$

$$b_2 = \frac{R_2(1 - S_2/R_1)x_1}{1 + (R_2 - 1)x_1 + (R_1 - 1)x_2} \tag{24}$$

$$c_1 = -(S_1 - 1)x_2 \tag{25}$$

$$c_2 = (S_1 - 1)x_1 + 1 \tag{26}$$

$$e_1 = \frac{R_2\,(1 - S_1/R_2)x_2}{1 + (R_2 - 1)x_1 + (R_1 - 1)x_2} \tag{27}$$

$$e_2 = \frac{R_2}{R_1}\,\frac{1 + (S_1 - 1)x_1 + (R_1 - 1)x_2}{1 + (R_2 - 1)x_1 + (R_1 - 1)x_2} \tag{28}$$

$$\frac{\rho}{\rho_\infty} = \frac{1 + (S_1 - 1)x_1 + (S_2 - 1)x_2}{1 + (S_1 - 1)x_{1\infty}} \tag{29}$$

$$S_1 = M_1/M_3; \quad S_2 = M_2/M_3 \tag{30}$$

$$R_1 = \mathcal{D}_{13}/\mathcal{D}_{12}; \quad R_2 = \mathcal{D}_{23}/\mathcal{D}_{12} \tag{31}$$

$$N_{Sc_{13}} = \nu_\infty/\mathcal{D}_{13} \tag{32}$$

Boundary Conditions

The straightforward boundary conditions on the momentum equations are:[7]

at $\xi = 0$,

$$F = 0, \quad G = 1 \tag{33}$$

at $\xi = \infty$,

$$F = 0, \quad G = 0 \tag{34}$$

The boundary condition on the axial velocity at the disk surface will be considered shortly.

The concentration of iodine in the bulk gas is specified, and that of GeI_4 is zero:

at $\xi = \infty$,

$$x_1 = x_{1\infty}, \quad x_2 = 0 \tag{35}$$

at the disk surface, the concentration of iodine is zero:

$$\text{at } \xi = 0, \quad x_1 = 0 \tag{36}$$

The concentration of GeI_4 at the surface, however, cannot be specified. Instead, a relation between the gradients of x_1 and x_2 at $z = 0$ must be obtained from the stoichiometry of the reaction, by which two moles of I_2 are consumed for every mole of GeI_4 produced. In terms of the mass fluxes relative to the disk surface, this yields:

$$\frac{n_{10}}{n_{20}} = -2\frac{M_1}{M_2} \tag{37}$$

The fluxes with respect to the mass average velocity (j_i) are related to the n_i by:

$$j_{20} = n_{20} - \rho_{20} w_0 = n_{20} - \omega_{20} \rho_0 w_0 \tag{38}$$

and

$$j_{10} = n_{10} \tag{39}$$

The mass average velocity at the surface is:

$$w_0 = \frac{n_{10} + n_{20}}{\rho_0} = \frac{n_{20}}{\rho_0} \left(1 - 2 \frac{M_1}{M_2}\right) \tag{40}$$

The ratio of the mass fluxes with respect to the mass average velocity at the interface is then:

$$\frac{j_{10}}{j_{20}} = - \frac{2M_1/M_2}{1 - \omega_{20}(1 - 2M_1/M_2)} \tag{41}$$

The fluxes j_{10} and j_{20} are obtained from Eqs. (6) and (7) and substituted into Eq.(41). With the necessary dimensionless transformations, the result is:

$$(g_0 b_{10} + e_{10}) \left(\frac{dx_1}{d\xi}\right)_0 = - e_{20} \left(\frac{dx_2}{d\xi}\right)_0 \tag{42}$$

where

$$g_0 = \frac{1}{2} \frac{1 + (2S_1 - 1)x_{20}}{1 + (S_2 - 1)x_{20}} \tag{43}$$

Equation (42) is the fourth boundary condition for the diffusion equations.

The surface boundary condition on the axial component of the velocity

can be obtained in a similar manner beginning from Eq. (40). This procedure yields*

$$H(0) = \frac{1}{N_{Sc_{13}}} \left\{ \frac{(\frac{1}{2} S_2 - S_1) b_{10}}{[1 + (S_2 - 1)x_{20}]^2} \right\} \left(\frac{dx_1}{d\xi} \right)_0 \tag{44}$$

The complete theoretical solution to the diffusion convection problem is the simultaneous solution of Eqs. (16) - (20) subject to the boundary conditions given by Eqs. (33) - (36), (42) and (44).

The desired result is the iodine flux at the interface, which is directly related to the measured rate of weight loss of the germanium disk. The former is:

$$\bar{n}_{10} = -\sqrt{\frac{\Omega}{\nu_\infty}} \frac{\mathcal{D}_{13} M_1 b_{10}}{RT\,[1 + (S_2 - 1)x_{20}]} \left(\frac{dx_1}{d\xi} \right)_0 \tag{45}$$

where the total concentration, C, has been written as 1/RT for an ideal gas at a total pressure of 1 atm. Before considering the full ternary diffusion problem, two limiting cases will be considered: a reactant gas consisting of dilute iodine in the inert carrier gas, and a pure iodine reactant.

The Dilute Gas Limit $x_{1\infty} \to 0$

In this case, the feed gases consist primarily of inert diluent with

---

* In Eq. (44) and the previous development, all velocities are mass averaged, while the concentration units are mole fractions. Most other analyses of the interfacial velocity effect,[3,5] utilize mass fraction units with mass average velocities. The B of ref. (3) and the ϵ_v of ref. (5) are equal to the term in the brackets of Eq. (44) multiplied by the conversion from mole fraction gradient to mass fraction gradient, which is $M_1 M_2 / \bar{M}_0^2$.

a small concentration of iodine; x_1 and x_2 and their gradients approach zero at all points.

In the momentum equations [Eqs. (16) - (18)] , the density ratios are all unity and the interfacial velocity boundary condition, Eq. (44), reduces to $H(0) = 0$. The momentum equations are completely decoupled from the diffusion equations. A numerical solution for the axial velocity, $H(\xi)$, is available.[7]

Taking the limit of the coefficients $a_1 \ldots e_2$, the diffusion equations become uncoupled from the momentum equations and from each other:

$$N_{Sc_{13}} H(\xi) \frac{dx_1}{d\xi} = \frac{d^2x_1}{d\xi^2} \tag{46}$$

$$N_{Sc_{23}} H(\xi) \frac{dx_2}{d\xi} = \frac{d^2x_2}{d\xi^2} \tag{47}$$

The iodine transfer rate can be obtained by solution of Eq. (46) subject to the boundary conditions given by the first part of Eq.(35) and Eq. (36). Equation (47) need not be considered unless a value of x_{20} is desired. The iodine flux expression, Eq. (45), reduces to:

$$n_{10} = -\sqrt{\frac{\Omega}{\nu_\infty}} \frac{\mathscr{D}_{13} M_1}{RT} \left(\frac{dx_1}{d\xi} \right)_0 \tag{48}$$

The numerical solutions to Eq. (46) using the tabulated values of $H(\xi)$ has been obtained previously for a large range of Schmidt numbers.[8] However, a sufficiently accurate analytical solution in the Schmidt number range of interest here ($1 \leq N_{Sc} \leq 3$) can be obtained by a linear approximation to the function $H(\xi)$:

$$H(\xi) = -\epsilon_{id}\xi \tag{49}$$

The subscript id denotes infinite dilution, where variable density and interfacial velocity effects are absent.

Figure 1 compares the exact velocity profile with the linear approximation, the slope of which has been chosen visually as 0.25. The solution of Eq. (46) with the velocity given by Eq. (49) is:

$$\left(\frac{dx_1}{d\xi}\right)_0 = \left(\frac{2\epsilon_{id}}{\pi}\right)^{1/2} N_{Sc_{13}}^{1/2} \; x_{1\infty} = 0.40 \; N_{Sc_{13}}^{1/2} \; x_{1\infty} \tag{50}$$

Equation (50) is less than 1% greater than the exact solution at a Schmidt number of unity and 11% high at a Schmidt number of 10. Its accuracy is well within the experimental precision for Schmidt numbers between one and three.

Despite the existence of an exact solution, the solution based upon the linear velocity profile has been used for comparison of theory with experiment for the following reasons: First, the dependence of the rate upon the experimental parameters is explicit and easily seen. Second, the linear velocity profile permits an estimation of the variable density effect to be made without resorting to machine computation. This calculation will be discussed later.

Inserting Eq. (50) into Eq. (48) and converting n_{10} to the rate of weight loss ($m = -n_{10}M_{Ge}A_{disk}\times 10^3/2M_1$), there results:

$$m = \left[\frac{1}{2}\left(\frac{2\epsilon_{id}}{\pi}\right)^{1/2} \frac{A_{disk}M_{Ge}\times 10^3}{R}\right] \frac{\mathcal{D}_{13}^{1/2}\,\Omega^{1/2}x_{1\infty}}{T} \tag{51}$$

The bracketed term in Eq. (51) is a numerical constant with a value of 505 mg-°K/cm for a 3/4" diameter Ge disk.

An interesting feature of Eq. (51) is that the rate is independent of the viscosity of the gas. This behavior is a direct consequence of the linear velocity profile.

Another characteristic of the above expression is that the rate is nearly temperature independent as well. The diffusivity of the Ar-I_2 system has been estimated from the gas kinetic theory method with force constants for the Lennard-Jones potential taken from viscosity data, (See Appendix B). This procedure yields a diffusion coefficient at 415°C of 0.34 cm^2/sec, and a temperature variation as $T^{1.81}$. The ratio $\mathcal{D}_{13}^{1/2}/T$ varies as $T^{-0.1}$, and the theoretical variation in m over the range 360°C-460°C is 3%. Since the precision of the data is at most 5%, this variation could not be observed. The constancy of rate with temperature in the diffusion limited regime is evident from Fig. 4 of the previous paper. At T = 415°C, Ω = 93 sec^{-1} and $x_{1\infty}$ = 0.126, the predicted rate is 0.52 mg/sec. The observed rate was 0.575±0.022 mg/sec over the range 360-460°C. The theoretical prediction is 9.6% low.

The variation of rate with disk speed is shown on Fig. 2 and compared to the prediction of Eq. (51). At speeds below 900 rpm, the discrepancy between theory and experiment is large and most probably due to natural convection effects. Above 900 rpm, the experimental rate follows the $\Omega^{1/2}$ prediction of Eq. (51). Again, the experimental data fall ~10% higher than the theory.

Equation (51) predicts that the rate should be directly proportional to the inlet iodine mole fraction. Although the concentration at which the effects of variable density, multicomponent diffusion and interfacial velocity begin to distort the linearity of the infinite dilution approximation is not known, Fig. 5 of the previous paper indicates a direct proportionality

between m and $x_{1\infty}$ up to $x_{1\infty} \approx 0.22$. The slope of the line through the experimental points is about 15% greater than the slope predicted by Eq. (51).

It has been demonstrated that the order of magnitude agreement between theory and experiment in the dilute iodine region is within 10-15%. The predicted dependence on disk speed, temperature, and iodine concentration also agree very well with theory. The effect of altering the diffusion coefficient while maintaining all other parameters constant (by changing the diluent from argon to helium) will be discussed later.

The agreement between theory and experiment in the dilute gas region substantiates the two major assumptions of the theoretical analysis: First, that the diffusional resistance is that predicted from the hydrodynamics of an infinite rotating disk; second, that the iodine concentration at the disk surface is zero. The 10-15% discrepancy between the measured and predicted rates can be due to many causes. The most probable is the effect of the protrusion of the disk above the holder, which adds ~16% to the total area of exposed germanium compared to the flat surface of the disk. However, the flow in the region of the edge should be relatively sluggish compared to that on the horizontal surface, and a full 16% increase in the mass transfer rate would not be expected. It is possible that at 900 rpm (where most of the data reported here were taken) there still exist residual natural convection effects which augment the forced convection mass transfer. Effects such as viscosity variations in the boundary layer and the accuracy of diffusion coefficient estimates may also contribute to the discrepancy.

In the analysis of transfer in concentrated iodine gases, the absolute value of the iodine flux at the disk surface will not be computed.

Instead, the flux per unit inlet iodine mole fraction divided by the same quantity as $x_{1\infty} \to 0$ in argon will be calculated. This ratio is defined as $\Gamma(x_{1\infty})$, and is a function of the inlet iodine mole fraction and the nature of the diluent gas:

$$\Gamma(x_{1\infty}) = \frac{(n_{10}/x_{1\infty})}{(n_{10}/x_{1\infty})_{x_{1\infty} \to 0, \mathrm{Ar}}} = \frac{(m/x_{1\infty})}{(m/x_{1\infty})_{x_{1\infty} \to 0, \mathrm{Ar}}} \tag{52}$$

The parameter Γ is effectively the ratio of the mass transfer coefficients in the concentrated and dilute reactant gas regions.

This method of comparing theory and experiment has been chosen for the following reasons: First, the geometrical and mechanical factors (such as the effect of the protruding edge of the disk) which contributed to the 10-15% discrepancy between theory and experiment in the dilute gas region are present in both numerator and denominator of Eq. (52) and tend to cancel; the ratio method isolates the effect due solely to alteration of the inlet gas composition (i.e., change of diffusion coefficient or multicomponent diffusion, variable density through the boundary layer, and interfacial velocity). Second, the denominator of Eq. (52) is experimentally well established by the slope of the line on Fig. 5 of the previous paper. Theoretically, the denominator of Eq. (52) is given by Eqs. (48) and (50):

$$\left(\frac{n_{10}}{x_{1\infty}}\right)_{x_{1\infty} \to 0, \mathrm{Ar}} = -\sqrt{\mathcal{D}_{13}\Omega}\left(\frac{M_1}{RT}\right)\left(\frac{2}{\pi}\right)^{1/2}\sqrt{\epsilon_{id}} \tag{53}$$

where $\mathcal{D}_{13}$ refers to the diffusion coefficient of iodine in argon.

The Binary Limit $x_{1\infty} \to 1$

In the limit as $x_{1\infty} \to 1$ the gas phase consists solely of a mixture of I_2 and GeI_4; the gas is pure iodine in the bulk and pure GeI_4 at the disk surface.

The diffusion equations are reduced by setting $x_1 + x_2 = 1$. Both Eqs. (19) and (20) become:

$$\frac{N_{Sc_{12}} H(\xi)}{\rho/\rho_\infty} \frac{dx_1}{d\xi} = \frac{d}{d\xi}\left[\frac{1}{\rho/\rho_\infty} \frac{dx_1}{d\xi}\right] \tag{54}$$

where the density term is:

$$\frac{\rho}{\rho_\infty} = \frac{M_2}{M_1} - \left(\frac{M_2}{M_1} - 1\right) x_1 \tag{55}$$

The ratio S_2/S_1 has been written as M_2/M_1.

The interfacial velocity boundary condition, Eq.(44) reduces to:

$$H(0) = \frac{\left(\frac{1}{2} - \frac{M_1}{M_2}\right)}{N_{Sc_{12}}} \left(\frac{dx_1}{d\xi}\right)_0 \tag{56}$$

The boundary conditions in the diffusion equation are:

$$x_1(0) = 0; \quad x_1(\infty) = 1 \tag{57}$$

Equations (16) - (18), and (54), subject to the boundary conditions given by Eqs. (33), (34), (56), and (57), are to be solved for $(dx_1/d\xi)_0$; the form of Eq. (45) appropriate to $x_{1\infty} = 1$ then gives the iodine transfer rate:

$$n_{10} = -\sqrt{\frac{\Omega}{\nu_\infty}} \quad \frac{\mathcal{D}_{12} M_1}{RT} \quad \left(\frac{dx_1}{d\xi}\right)_0 \tag{58}$$

This equation is then used in Eq. (52) to give Γ (1).

Rather than attempt a direct numerical solution of the coupled momentum, overall continuity and diffusion equations, an approximate solution will be obtained by dividing up the problem into more tractable slices.

The ratio $\Gamma(1)$ differs from unity for three reasons:

(1) the density ratio in the momentum and overall continuity equations is no longer unity, and for this reason, the axial velocity profile can not be represented by the constant property formula, Eq. (49).

(2) the interfacial velocity boundary condition [H(0)] is not zero, as with dilute iodine reactant gases but is given by Eq. (56). This will also alter the velocity profile and consequently the transfer rate.

(3) aside from the density effect on $H(\xi)$, there is a direct effect of the variable density in the diffusion equation, Eq. (54). In addition, the diffusivity in Eq. (54) is that of iodine in GeI_4 rather than iodine in argon.

To approximate the effect of variable density in the momentum and overall continuity equations, the axial velocity, $H(\xi)$, is obtained from Eqs. (16) - (18) with the boundary condition $H(0) = 0$ and the dependence of the density upon axial position determined from the solution of the binary, infinite dilution diffusion equation. As before, the resulting profile is approximated by:

$$H(\xi) = -\epsilon\xi \tag{59}$$

However, the slope ϵ is in general different from the constant density value, ϵ_{id}.

The effect of interfacial velocity is approximated from the simultaneous solution of Eqs. (16) - (18) and (54) wherein ρ/ρ_∞ is set equal to unity. Equation (56) is used as the axial velocity boundary condition. The solution to this type of problem, in which the term $(1/2-M_1/M_2)$ in Eq. (56) is denoted by B or ϵ_V, has been obtained previously for flat plate[3] and rotating disk geometries.[5]

The third factor is obtained from a solution of Eq.(54), with $H(\xi)$ given by Eq.(59) and ρ/ρ_∞ given by Eq.(55).

Each of the three contributing factors is determined without regard to the perturbations engendered by the other two. This particular method of decoupling the conservation equations was chosen in an attempt to avoid a complete numerical solution, yet retain the essential features of the three major effects. For example, in the estimation of the effect of variable density in the flow equations, the true density variation is probably not far from that given by the infinite dilution solution. Using even a rough estimate of ρ/ρ_∞ is at least preferable to setting this ratio equal to unity. An additional advantage of this method is that the magnitudes of the three effects are seen immediately, a feature which would be absent in the numerical solution of the full set.

For a pure iodine reactant gas, the third factor can be obtained by inserting Eqs. (55) and (59) into Eq. (54) and defining a new concentration variable:

$$X_1 = \frac{\ln\left[\frac{M_2}{M_1} - \left(\frac{M_2}{M_1} - 1\right) x_1\right]}{\frac{M_2}{M_1} - 1} \tag{60}$$

Equation (54) is reduced to:

$$-\epsilon N_{Sc_{12}} \frac{dX_1}{d\xi} = \frac{d^2X_1}{d\xi^2} \tag{61}$$

and the boundary conditions, Eq. (57), become:

$$X_1(0) = \frac{\ln (M_2/M_1)}{\frac{M_2}{M_1} - 1} \quad ; \quad X_1(\infty) = 0 \tag{62}$$

The solution (in terms of the original mole fraction variable) is:

$$\left(\frac{dx_1}{d\xi}\right)_0 = \frac{\frac{M_2}{M_1} \ln\left(\frac{M_2}{M_1}\right)}{\frac{M_2}{M_1} - 1} \left(\frac{2}{\pi}\right)^{1/2} \sqrt{\epsilon N_{Sc_{12}}} \tag{63}$$

The first term on the right has previously been obtained by Hanna.[4] A similar treatment of the variable density diffusion equation has also been given by Bedingfield and Drew.[1]

The solution to the infinite dilution (or constant property) conservation equation for a rotating disk with an interfacial velocity boundary condition given by Eq. (56) is presented graphically in Ref. 6, in which the ratio of the concentration gradient at the surface with the interfacial velocity boundary conditions to that with $H(0) = 0$ is plotted as a function of Schmidt number for various values of the interfacial velocity parameter ϵ_v (equal to $1/2-M_1/M_2$ in the present study). Here the gradient ratio will be denoted by F_2 and the interfacial velocity parameter as B rather than ϵ_v, to conform to the notation which has been utilized most frequently in flat plate studies of the same problem. A

cross-plot of the results of Ref. 6 is presented in Fig. 3, where it is seen that F_2 is nearly independent of Schmidt number for B values near unity.

The gradient at the disk surface which includes all of the pertinent effects is F_2 times the gradient given by Eq. (63). When this product is inserted into Eq. (58) and this equation and Eq. (53) inserted into Eq. (52), the final result is:

$$\Gamma(1) = \sqrt{\frac{\epsilon}{\epsilon_{id}}}\, F_2 \left[\left(\frac{\mathcal{D}_{12}}{\mathcal{D}_{13}} \right)^{1/2} \cdot \frac{M_2/M_1 \ln (M_2/M_1)}{M_2/M_1 - 1} \right] \tag{64}$$

The first term on the right is the effect of density variation in the flow equations, and will be denoted by F_1:

$$F_1 = \sqrt{\epsilon/\epsilon_{id}} \tag{65}$$

The second term reflects the effect of interfacial velocity. The third term (in brackets) is the effect of the different diffusion coefficient and variable density in the diffusion equation. It will be denoted by F_3.

In Appendix A, the momentum integral method is used to obtain an estimate of the ratio ϵ/ϵ_{id}, which depends upon the parameters:

$$\beta = \rho_0/\rho_\infty - 1 \tag{66}$$

and

$$\Phi = \delta_{id}/\delta_D \tag{67}$$

The ratio ρ_0/ρ_∞ is obtained from the average molecular weights at the surface and in the bulk. δ_{id} is the flow boundary layer thickness for the constant property, zero interfacial velocity system and is equal to 2.56. δ_D is the thickness of the diffusion boundary layer in the dilute gas system and is given by:

$$\delta_D = (48/N_{Sc_{12}})^{1/2} \tag{68}$$

Thus

$$\Phi = 0.37\sqrt{N_{Sc_{12}}} \tag{69}$$

The rate of germanium loss has been measured at 415°C and 900 rpm with pure iodine inlet gas. Based on three measurements, the rate was 3.36±0.08 mg/sec. The denominator of Eq. (52) is based upon the five points along the line of Fig. 5 of the previous paper, and has a value of 4.78±0.15 mg/sec-unit mole fraction I_2. The experimental value of $\Gamma(1)$ is thus:

$$\Gamma(1)_{exp} = 0.70 \pm 0.03$$

Using the values of the diffusion coefficients of iodine in argon and iodine in GeI_4 given in Appendix B, the diffusivity term in Eq. (64) is:

$$\left(\frac{\mathcal{D}_{12}}{\mathcal{D}_{13}}\right)^{1/2} = 0.41$$

The ratio of the molecular weights of GeI_4 to I_2 is 2.287 and the term involving M_2/M_1 in Eq.(64) is 1.47. The factor F_3 is 0.60.

The interfacial velocity factor, F_2, is obtained from Fig. 3 with a value of $B = 1/2 - M_1/M_2 = 0.063$. The value of F_2 is 0.97.

The density ratio in Eq. (66) is equal to the molecular weight ratio of 2.287 and β is 1.287. The Schmidt number of iodine in GeI_4 (assuming the viscosity of the mixture, regardless of composition, to be that of pure iodine) is ~1.3 and the parameter Φ is 0.42. According to the method developed in Appendix A, the ratio ϵ/ϵ_{id} is 1.46 and the factor F_1 is 1.21. The ratio $\Gamma(1)$ as calculated by the theory presented here is the product of F_1, F_2, and F_3:

$$\Gamma(1)_{calc} = (1.21)\ (0.97)\ (0.60) = 0.70$$

The excellent agreement between the experimental and theoretical values of $\Gamma(1)$ is in part fortuitous; although the accuracy of the calculational method is not known, there is bound to be some error due to the arbitrary uncoupling of the conservation equations and due to the approximate method of treating the effect of density variation in the flow equations. For the case of pure iodine inlet gas, the errors apparently cancel.

If the density variation and interfacial velocity effects had been neglected entirely, and the GeI_4-I_2 system considered as a constant property binary, the predicted value of $\Gamma(1)$ would simply have been the square root of the diffusivity ratio; such a calculation would have been in error by nearly a factor of two (0.41 instead of 0.70).

In this instance, the density variation acts very strongly to accelerate the transfer rate. An increase of 47% results from the density term in the diffusion equation and an increase of 21% due to the density variation in the flow equations.

The effect of interfacial velocity is small, causing only a 3% reduction in the transfer rate. The correction factor is less than unity

because the mass average velocity at the disk is directed away from the surface; one mole of GeI_4 leaves the surface for each two moles of iodine which are brought in. Because of the germanium picked up by the two moles of iodine, the mass of material leaving the surface is slightly greater than that arriving. However, since the mass of a single germanium atom is small compared to that of 4 iodine atoms, the effect is not large. The effect would be much greater if, for example, metallic lead were subject to attack by fluorine.

Recently, Hanna has derived a formula for estimating the effect of variable density and interfacial velocity in gas phase mass transfer at Schmidt number near unity (Eq. (36) of Ref. 3). Using the molecular weights, surface and bulk concentrations, and the molar flux ratio at the surface characteristic of the system in this study, Hanna's expression is:

$$\frac{\left[\dfrac{\ln(1-\frac{1}{2})}{-(\frac{1}{2})}\right]^{4/3}\left[\dfrac{1.287}{e^{1.287}-1}\right]^{1/3}}{\left[1+\frac{4}{21}\ln(1-\frac{1}{2}\right]^{4/9}} = 1.30$$

Since this expression is for constant diffusivity, it must be corrected for the difference in diffusion coefficient between the I_2-Ar and I_2-GeI_4 system. This is the factor 0.41 presented earlier. The estimate of $\Gamma(1)$ by Hanna's method yields:

$$\Gamma(1)_{Hanna} = (1.30)\ (0.41) = 0.53$$

This correction is considerably lower than the experimental value of 0.70.

The Ternary Range $0 < x_{1\infty} < 1$

Between the two limiting cases of dilute iodine and pure iodine reactant gases, the multicomponent nature of I_2-GeI_4-diluent mixture cannot be avoided. In the following treatment, the calculational procedure developed for the case of pure iodine will be employed. The ratio $\Gamma(x_{1\infty})$ of Eq. (52) will be determined by independent consideration of the effects of density variation in the flow equations, interfacial velocity, and density variation and multicomponent effects in the diffusion equations.

The major difference between the analysis of the three component system and the I_4-GeI_4 binary is the third factor; instead of a single diffusion equation, there are now two, and the effect of the altered diffusional characteristics cannot be expressed as a simple diffusivity ratio, as it was in the pure iodine case.

A new axial distance variable is defined:

$$\eta = \left(\frac{1}{2}\,\epsilon\, N_{Sc_{13}}\right)^{1/2} \xi \tag{70}$$

with the axial velocity approximated by Eq. (59), the diffusion equations, Eqs. (19) and (20) become:

$$-\frac{2\eta}{\rho/\rho_\infty}\left(a_1\frac{dx_1}{d\eta} + a_2\frac{dx_2}{d\eta}\right) = \frac{d}{d\eta}\left[\frac{1}{\rho/\rho_\infty}\left(b_1\frac{dx_1}{d\xi} + b_2\frac{dx_2}{d\xi}\right)\right] \tag{71}$$

and

$$-\frac{2\eta}{\rho/\rho_\infty}\left(c_1\frac{dx_1}{d\eta} + c_2\frac{dx_2}{d\xi}\right) = \frac{d}{d\eta}\left[\frac{1}{\rho/\rho_\infty}\left(e_1\frac{dx_1}{d\xi} + e_2\frac{dx_2}{d\xi}\right)\right] \tag{72}$$

where ρ/ρ_∞ is given by Eq. (29). The boundary conditions are given by Eqs. (35), (36), and (42) (in the last of these, ξ is replaced by η)..

Equations (71) - (72) have been solved by machine computation for $(dx_1/d\eta)_0$ and x_{20}, as functions of $x_{1\infty}$ for both argon and helium diluents. The iodine surface flux is obtained from Eq. (45), which in terms of η is:

$$\frac{\mathcal{N}_{10}}{x_{1\infty}} = -\sqrt{\mathcal{D}_{13}\Omega}\left(\frac{M_1}{RT}\right)\frac{b_{10}}{1+(S_2-1)x_{20}}\left(\frac{\epsilon}{2}\right)^{1/2}\frac{1}{\chi_{1\infty}}\left(\frac{dx_1}{d\eta}\right)_0 \quad (73)$$

Equations (53) and (73) are substituted into Eq. (52) and multiplied by the interfacial velocity factor, F_2, there results:

$$\Gamma(x_{1\infty}) = \sqrt{\frac{\epsilon}{\epsilon_{id}}}\; F_2\left[\frac{\sqrt{\pi}}{2}\;\frac{b_{10}}{1+(S_2-1)x_{20}}\;\frac{1}{x_{1\infty}}\left(\frac{dx_1}{d\eta}\right)_0\right] \quad (74)$$

The term in the brackets in Eq. (74) is the factor F_3, which varies from unity at $x_{1\infty} = 0$ in argon to 0.60 at $x_{1\infty} = 1$. With helium as diluent, Eq. (74) must be multiplied by the square root of the ratio of the diffusivity of iodine in helium to iodine in argon to account for the fact that the "3" in $\mathcal{D}_{13}$ of Eq. (73) refers to helium, whereas in Eq. (53), it refers to argon, which has been used as a reference gas. With helium, F_3 decreases from 2.18 at $x_{1\infty} = 0$ to 0.60 at $x_{1\infty} = 1$.

The first term on the right of Eq. (74) is the factor F_1, which has been computed by the same procedure as was used for pure iodine reactant. In the present case, the value of ρ_0/ρ_∞ required for the computation of β by Eq. (66) has been calculated from Eq. (29) with $x_{10} = 0$ and x_{20} given by the solution to two diffusion equations. The value of the Schmidt number for Eq. (69) has been approximated by:

$$\sqrt{N_{Sc}} = x_{1\infty}\sqrt{N_{Sc_{12}}} + (1 - x_{1\infty})\sqrt{N_{Sc_{13}}} \tag{75}$$

This approximation was chosen because it yieldsthe correct limits as $x_{1\infty}$ goes to zero and unity. Use of Eq (75) as an interpolation formula is considered a satisfactory means of estimating the parameter Φ since the factor F_1 is only weakly dependent upon Φ and all Schmidt numbers lie between 1 and 3.

The factor F_2, representing the effect of interfacial velocity, is furthest from unity for pure iodine reactant, where it has a value of 0.97. For simplicity, values in the region $0 \leq x_{1\infty} \leq 1$ have been approximated by:

$$F_2 = 1 - 0.03\, x_{1\infty} \tag{76}$$

The calculated values of $\Gamma(x_{1\infty})$ are shown in Table I as a function of $x_{1\infty}$ for argon and helium diluents. A comparison of the calculated values from Table I with the experimental results is shown in Fig. 4. The confidence limits shown on the plot represent the precision of duplicate results.

Except for the limit $x_{1\infty} = 1$, the theoretical results are 7-10% lower than the experimental points. This is probably the result of the approximate values of the theoretical calculation, especially the method of uncoupling of the conservation equations. The calculated effect of density variation in the flow equations (the factor F_1) is not as firmly grounded in the multicomponent region as is the $x_{1\infty} = 1$ binary. In the former, the density profile characteristic of a binary system [Eq. (A-7) with ρ_0/ρ_∞ obtained using the computer results for x_{20}] has been employed. Equation (A-7) may underestimate the density of the ternary system in the boundary layer, since the multicomponent effects undoubtedly make the

variation of average molecular weight (or density) with distance considerably more complex than in a binary system.

The deviation between theory and experiment cannot be reasonably attributed to failure of the Maxwell-Stephan equations upon which the two diffusion equations are based. The Maxwell-Stephan relations have been verified many times in pure molecular diffusion systems.

Another possibility is that the experimentally determined value of the denominator of Eq. (52) is in error. A value based upon the region $0 \leq x_{1\infty} \leq 0.20$ from Fig. 5 of the previous paper has been used, since all of the points on this plot appeared to fall on a single straight line. It is possible that the slope so obtained is lower than the desired limit as $x_{1\infty} \rightarrow 0$, because the experiments have not been extended sufficiently deep into the infinite dilution region to give a reliable limiting value of the ratio $m/x_{1\infty}$. If this is so, the experimental denominator is too small; were it ~10% larger than the value used here, all of the experimental ternary points would lie quite close to the theoretical line. The computed $\Gamma(1)$ (pure iodine), however, would then be 7-10% too high.

The agreement, however, is considered satisfactory, in view of the precision of the experiments and the approximations involved in the theoretical analysis.

The only other theoretical method for estimating the effect of multicomponent diffusion on the rate of mass transfer has been presented by Toor.[10] This method emphasizes the multicomponent diffusion effects, but does not consider interfacial velocity or density changes, either in the flow equations or in the diffusion equations. This method has been applied to the system for which $x_{1\infty} = 0.5$ in argon (details in Appendix C), and predicts a value of x_{20} of 0.36, compared to 0.42 obtained by numerical solution

of the diffusion equations [Eqs. (71) and (72)]. The value of $\Gamma(0.5)$ predicted by Toor's method is 0.65. The theory presented in the study predicts a value of 0.81 and the experimental value is 0.89 ± 0.04. The discrepancy in the case of Toor's calculation is most probably due to not accounting for density effects and, to an unknown extent, to considering the practical diffusion coefficients as constants.

Table I. Calculated Correction Factors for Transfer in the Ternary Range

$x_{1\infty}$	x_{20}	F_1	F_2	F_3	Γ
		ARGON			
0	0	1.00	1.00	1.00	1.00
0.10	0.067	1.05	1.00	0.91	0.96
0.25	0.184	1.10	0.99	0.82	0.89
0.50	0.42	1.16	0.98	0.71	0.81
0.75	0.69	1.18	0.98	0.64	0.74
1.00	1.00	1.21	0.97	0.60	0.70
		HELIUM			
0	0	1.00	1.00	2.18	2.18
0.10	0.074	1.14	1.00	1.40	1.60
0.25	0.21	1.18	0.99	1.03	1.20
0.50	0.46	1.20	0.98	0.78	0.92
0.75	0.72	1.21	0.98	0.66	0.79

NOMENCLATURE

a_1, a_2	Defined by Eqs. (21) and (22).
A_{disk}	Surface area of disk, cm^2.
b_1, b_2	Defined by Eqs. (23) and (24).
B	Interfacial velocity parameter, equal to $1/2 - M_1/M_2$.
c_1, c_2	Defined by Eqs. (25) and (26).
C	Total concentration, gm-mole/cm^3.
$\mathcal{D}_{ij}$	Binary diffusion coefficient for ij pair, cm^2/sec.
D_{ij}	Multicomponent diffusion coefficients defined by Eq. (7), cm^2/sec.
D_{ij}^m	Practical diffusion coefficients defined by Eqs. (C-3) and (C-4), cm^2/sec.
D_i^m	Diffusion coefficient used in Toor's method, cm^2/sec.
e_1, e_2	Defined by Eqs. (27) and (28)
F	Dimensionless radial velocity, Eq. (11).
F_1	Factor representing the effect of density variation in the momentum and overall continuity equations on the rate, Eq.(65).
F_2	Factor representing the effect of interfacial velocity on the rate.
F_3	Factor representing the effect of density variations and multicomponent diffusion in the diffusion equations on the rate.
G	Dimensionless tangential velocity, Eq. (12).
g_o	Defined by Eq. (43).
H	Dimensionless axial velocity, Eq. (13).
j_i	Mass flux of component i relative to the mass average velocity, gm/cm^2 - sec.
k	Boltzman constant.
m	Rate of weight loss of disk, mg/sec.

M	Molecular weight.
M_{Ge}	Atomic weight of germanium.
n_{io}	Mass flux of component i at disk surface, gm/cm^2 - sec.
N_{Sc}	Schmidt number.
Q_A, Q_B, Q_C, Q_δ, Q_ϵ	Functions of Φ in momentum integral method.
r	Radial distance along disk, cm.
R_1, R_2	Diffusivity ratios, Eq. (31).
R	Gas constant, cm^3 - atm/gm mole - °K.
S_1, S_2	Molecular weight ratios, Eq. (30).
T	Temperature, °K.
T_b	Boiling point, °K.
u	Radial velocity component, cm/sec.
v	Tangential velocity component, cm/sec.
V_b	Molar volume at boiling point, $Å^3$.
w	Axial velocity component, cm/sec.
x	Mole fraction.
X_1	Concentration variable defined by Eq. (60).
y	Dimensionless distance, Eq. (A-13).
z	Axial distance from disk, cm.

GREEK LETTERS

Φ Ratio of flow to diffusion boundary layer thicknesses.

ρ Density, gm/cm^3.

ρ_i Mass concentration of component, gms i/cm^3.

μ Viscosity gm/cm-sec.

Ω Disk rotational speed, sec^{-1}.

ω Mass fraction.

ξ Dimensionless axial distance, Eq. (15).

ν Kinematic viscosity, cm^2/sec.

ϵ Slope of linear approximation of axial velocity profile; also force constant in Lennard-Jones potential.

Γ Ratio defined by Eq. (52).

β Defined by Eq. (66).

δ Flow boundary layer thickness (in units of ξ).

δ_D Diffusion boundary layer thickness (in units of ξ).

η Dimensionless variable defined by Eq. (70).

α Defined by third of Eqs. (A-17).

σ Collision diameter in Lennard-Jones Potential, Å.

SUBSCRIPTS

1 Iodine

2 GeI_4

3 Diluent

0 Disk surface ($\xi = 0$)

∞ Bulk gas ($\xi = \infty$)

id Infinite dilution, (constant properties, zero interfacial velocity)

SUPERSCRIPTS

' Differentiation with respect to ξ

REFERENCES

1. Bedingfield, C. H. and T. B. Drew, Ind. Eng. Chem., 42, 1164 (1950).
2. Bird, R. B., W. E. Stewart, and E. N. Lightfoot, Transport Phenomena, John Wiley and Sons, New York (1964).
3. Hanna, O. T., AIChE Journal, 11, 706 (1965).
4. Hanna, O. T., AIChE Journal, 8, 278 (1962).
5. Olander, D. R., Int. J. Heat and Mass Trans., 5, 765 (1962).
6. Olander, D. R., ASME J. Heat Trans., 84C, 185 (1962).
7. Schlichting, Hermann, Boundary Layer Theory, 4th Edition, p. 83, McGraw-Hill Book Co., New York (1960).
8. Sparrow, E. M. and J. L. Gregg, Jl. Heat Trans., 81C, 249 (1959).
9. Sherwood, T. K. and R. C. Reid, The Properties of Gases and Liquids, McGraw-Hill Book Co., New York (1958).
10. Toor, H. L., AIChE Journal, 10, 448 (1964).
11. Toor, H. L., AIChE Journal, 8, 561 (1962).
12. Van Karman, T., Zeit. fur Ang. Math and Mech., 1, 233 (1921) (See also NACA TM 1092).

APPENDIX A - Momentum Integral Method for Estimating the Effect of Density Variation on the Axial Velocity

In order to solve Eqs. (16) to (18) for the velocity component $H(\xi)$, an estimate of the variation of the density with distance is required. This will be obtained by a momentum integral solution of Eq. (54) in which the effects of density variation are neglected and the axial velocity profile is approximated by Eq. (49). Equation (54) reduces to:

$$- \epsilon_{id} N_{Sc_{12}} \xi \frac{dx_1}{d\xi} = \frac{d^2 x_1}{d\xi^2} \qquad \text{(A-1)}$$

subject to boundary conditions given by Eq. (57). In addition, a diffusion boundary layer of thickness δ_D (in dimensionless units) is assumed, at which point

$$\left(\frac{dx_1}{d\xi}\right)_{\delta_D} = 0 \qquad \text{(A-2)}$$

In addition, Eq. (A-1) also requires that at $\xi = 0$:

$$\left(\frac{d^2 x_1}{d\xi^2}\right)_0 = 0 \qquad \text{(A-3)}$$

Assuming a cubic concentration profile, the four conditions provided by Eqs. (57),(A-2) and (A-3) yield:

$$x_1 = 1 - \left(1 - \xi/\delta_D\right)^3 \qquad \text{(A-4)}$$

If this expression is inserted in the left hand derivative of Eq. (A-1), the entire equation integrated from $\xi = 0$ to $\xi = \delta_D$, and the gradient at $\xi = \delta_D$ set equal to zero according to Eq. (A-2), the diffusion boundary layer thickness is found to be:

$$\delta_D = \left(\frac{12}{\epsilon_{id} N_{Sc_{12}}}\right)^{1/2} = \left(\frac{48}{N_{Sc_{12}}}\right)^{1/2} \tag{A-5}$$

For a constant temperature binary mixture, the density function implied by Eq. (A-4) is obtained by noting that:

$$\rho = \bar{M}C = [M_2-(M_2-M_1)x_1]\ C$$

$$\rho_0 = M_2 C; \quad \rho_\infty = M_1 C \tag{A-6}$$

This yields:

$$\frac{\rho}{\rho_\infty} = 1 + \left(\frac{\rho_0}{\rho_\infty} - 1\right)\left(1 - \frac{\xi}{\delta_D}\right)^3 \tag{A-7}$$

A measure of the accuracy of this solution can be obtained by computing the gradient at the surface from Eqs. (A-4) and (A-5):

$$\left(\frac{dx_1}{d\xi}\right)_0 = 0.867\left(\epsilon_{id} N_{Sc_{12}}\right)^{1/2} \tag{A-8}$$

The exact solution yields the same form of equation, except that the numerical constant in Eqs. (A-8) is $(2/\pi)^{1/2} = 0.798$. The momentum integral method overestimates the transfer rate by 8.6%.

The effect of neglecting the density ratio in Eq. (54) in obtaining Eq. (A-7) can be assessed by comparing Eq. (A-7) to the solution of Eq. (61), in which the ρ/ρ_∞ term has been incorporated into the variable X_1. The exact solution of Eq. (61) is:

$$\ln\left(\frac{\rho}{\rho_\infty}\right) = \ln\left(\frac{\rho_0}{\rho_\infty}\right)\left\{1-\mathrm{erf}\left[\left(\frac{\epsilon N_{Sc_{12}}}{2}\right)^{1/2}\xi\right]\right\} \tag{A-9}$$

A momentum integral solution to Eq. (61) can also be obtained as:

$$\frac{\rho}{\rho_\infty} = \exp\left\{\ln\left(\frac{\rho_0}{\rho_\infty}\right)\left(1 - \frac{\xi}{\delta_D}\right)^{1/3}\right\} \tag{A-10}$$

where δ_D is again given by Eq. (A-5) with ϵ_{id} replaced by ϵ. Note that Eq. (A-7) is the first term in the Taylor series expansion of Eq. (A-10).

A direct comparison of Eq. (A-9) and (A-10) with Eq. (A-7) cannot be made, since the parameter ϵ is not yet known (ϵ is the end result of the solution of the flow equations, for which we are now seeking an appropriate density function). However, if ϵ in Eqs. (A-9) and (A-10) is approximated by ϵ_{id}, the three expressions can be compared; the results are shown in Fig. 5 for $N_{Sc} = 1$, $\rho_0/\rho_\infty = 2$. This plot suggests that Eq. (A-7) overestimates the density at all points in the boundary layer. Nevertheless, it is clear that Eq. (A-7) is a better representation of the density variation with distance than a uniform value of unity.

The momentum integral solution of the momentum and overall continuity equations follows the original computation of Von Karman[12] except that density variation according to Eq. (A-7) is included. For the variable density case, the equivalent of Von Karman's Eq. (26) is:

$$3 \int_0^1 \left(\frac{\rho_0}{\rho_\infty}\right) F^2(y)\, dy - \int_0^1 \left(\frac{\rho}{\rho_\infty}\right) G^2(y)\, dy = - \frac{1}{\delta^2} \left(\frac{dF}{dy}\right)_0 \qquad \text{(A-11)}$$

$$4 \int_0^1 \left(\frac{\rho}{\rho_\infty}\right) F(y)G(y)\, dy = - \frac{1}{\delta^2} \left(\frac{dG}{dy}\right)_0 \qquad \text{(A-12)}$$

where δ is the flow boundary layer thickness and

$$y = \xi/\delta \qquad \text{(A-13)}$$

In terms of the distance variable y, the density ratio employed in Eqs. (A-11) and (A-12) is:

$$\frac{\rho}{\rho_\infty} = 1 + \beta\,(1 - \Phi\, y)^3 \qquad \text{(A-14)}$$

where

$$\beta = \frac{\rho_0}{\rho_\infty} - 1 \tag{A-15}$$

$$\Phi = \delta/\delta_D \tag{A-16}$$

Since Eq. (A-14) is valid only for $\Phi y \leq 1$ and the integrations in Eq. (A-11) and (A-12) extend to $y = 1$, it is necessary that $\Phi \leq 1$. For a Schmidt number of unity, $\delta_D = 6.93$ by Eq. (A-5). Since $\delta_{id} = 2.56$ for the constant density case, there is no problem in satisfying the condition $\Phi \leq 1$.

Following Von Karman, a fourth order polynomial in y is assumed for F(y). The five constants are determined by:

$F(0) = 0$	(from original boundary condition)	
$\left(\frac{d^2F}{dy^2}\right)_0 = -1$	(from differential equation with $F(1)=0$, $H(0) = 0$, $G(0) = 1$)	
$\left(\frac{dF}{dy}\right)_0 = \alpha$	(constant to be determined)	
$F(1) = 0$	(from original boundary condition)	
$\left(\frac{dF}{dy}\right)_1 = 0$	(auxillary condition)	(A-17)

The yields:

$$F(y) = y\,(1-y)^2\,[\alpha + (2\alpha - \tfrac{1}{2})y\,] \tag{A-18}$$

Similarly, the four constants for the cubic approximation to G(y) are obtained from:

$G(0) = 1$ (original boundary condition)

$$\left(\frac{d^2G}{dy^2}\right)_0 = 0 \qquad \text{(from differential equation with } H(0) = 0,\ F(0) = 0\text{)}$$

$$G(1) = 0 \qquad \text{(original boundary condition)} \qquad \text{(A-19)}$$

$$\left(\frac{dG}{dy}\right)_1 = 0 \qquad \text{(auxillary condition)}$$

This yields:

$$G(y) = \frac{1}{2}(2-3y + y^3) \qquad \text{(A-20)}$$

Equations (A-14), (A-18) and (A-20) are substituted into Eqs. (A-11) and (A-12) the integration and differentiations are performed. This yields two algebraic equations which must be solved for the unknowns α and δ in terms of the density variation parameters β and Φ. In conformity with the concept of using known infinite dilution results to generate the input parameters for the density variation, the flow boundary layer thickness δ in Eq. (A-16) is not treated as an unknown but is assigned the constant density value of $\delta_{id} = 2.56$. The results indicate that this is a satisfactory approximation, since α and δ are slowly varying functions of β and Φ.

After considerable manipulation, the solution can be put in the form:

$$\alpha = 0.964\left[\frac{1+\beta\ Q_C(\Phi)}{1\ \beta\ Q_A(\Phi)}\right]^{1/2} + 0.070\left[\frac{1+\beta\ Q_B(\Phi)}{1+\beta\ Q_A(\Phi)}\right] \qquad \text{(A-21)}$$

$$\delta = \frac{2.563}{[(\alpha/\alpha_{id})\ [1+\beta\ Q_\delta(\Phi)]]^{1/2}} \qquad \text{(A-22)}$$

From the present computation, the constant density values of α and δ are:

$$\alpha_{id} = 1.034$$

$$\delta_{id} = 2.56$$

Von Karman obtained 1.026 and 2.58 for α_{id} and δ_{id} respectively.

The functions $Q_A(\Phi)....Q_\delta(\Phi)$ are polynominals in Φ which arise in the course of the calculation. They are plotted in Fig. 6.

The axial velocity, H(y) can be obtained by integration of Eq. (18):

$$H(y) = -\frac{2\delta}{\rho/\rho_\infty} \int_0^y \left(\frac{\rho}{\rho_\infty}\right) F(y')\, dy' \qquad \text{(A-23)}$$

where ρ/ρ_∞ is given by Eq. (A-14) and F(y) by Eq. (A-18). The constants α and δ are given by Eqs. (A-21) and (A-22).

For $\beta = 0$ (constant density), $H_{id}(y)$ is given by:

$$H_{id}(y) = -2(2.563)[0.5170y^2-0.1667y^3-0.5255y^4+0.3136y^5] \qquad \text{(A-24)}$$

where $\xi = 2.563y$

For the system with pure iodine in the bulk and pure GeI_4 at the surface, $N_{Sc_{12}} \approx 1.3$ (assuming the viscosity to be that of pure iodine), $\Phi = 0.42$ and $\beta = 1.287$. Using Eqs. (A-21) and (A-22), these parameters yield $\alpha = 1.094$ and $\delta = 1.843$. The axial velocity is given by the function:

$$H(y) = -2(1.843)[1.2510y^2-0.9726y^3-0.9158y^4+1.4232y^5-0.7074y^6 + 0.1953y^7-0.0201y^8]/[1+1.287(1-042y)^3] \qquad \text{(A-25)}$$

where $\xi = 1.843y$

Equations (A-24) and (A-25) are plotted on Fig. 7.

Rather than employ the entire Eq. (A-25) in the diffusion equation, the velocity profiles are approximated by a straight line, as in the treatment of the dilute gas limit:

$$H(\xi) = -\epsilon\xi \tag{A-26}$$

where ϵ is approximated by the ratio of the velocity at the edge of the flow boundary layer to the thickness of the flow boundary layer:

$$\epsilon = -H(\delta)/\delta \tag{A-27}$$

These approximations are also shown on Fig. 7. The value of ϵ_{id} computed by this method is 0.277, compared to the value of 0.25 obtained by visual fitting of the exact solution. However, despite the 10% discrepancy between the exact and momentum integral figures for ϵ_{id}, the ratio ϵ/ϵ_{id}, in which both slopes are calculated by the momentum integral method, should be a reasonably accurate estimation of the true ratio. This ratio is given by:

$$\frac{\epsilon}{\epsilon_{id}} = \left(\frac{\alpha}{\alpha_{id}}\right)\left[1 + \beta\, Q_\epsilon(\Phi)\right] \Big/ \left[1 + \beta(1-\Phi)^3\right] \tag{A-28}$$

The function $Q_\epsilon(\Phi)$ is plotted on Fig. 6.

APPENDIX B - Physical Properties at 415°C

The primary physical properties required are the diffusion coefficients of the binary pairs included in the ternary system I_2-GeI_4-diluent.

Diffusion coefficients have been estimated from kinetic theory by the method of Hirschfelder, which is based upon the Lennard-Jones potential. The force constants for the potential have been obtained from gas phase viscosity data for Ar, He, and I_2, and are tabulated in Ref. 9. For GeI_4, the force constants have been estimated by

$$\sigma = 1.18\ V_b^{1/3} \qquad \text{(B-1)}$$

$$\epsilon/k = 1.21\ T_b \qquad \text{(B-2)}$$

The molar volume of GeI_4 has been taken as the sum of the estimated molar volumes of Ge and two I_2. The molar volume of Ge has been assumed equal to that of Br (which is 27) since the two have similar atomic weights. The molar volume of I_2 has been taken as 68; the molar volume of GeI_4 is estimated as 163, and from Eq. (B-1), the collision diameter is 6.45Å.

No boiling point for GeI_4 is available, since the material sublimes at atmospheric pressure. An effective "boiling point" has been estimated by assuming the ratio of the "boiling" to melting points of GeI_4 to be the same as the tetrahalides of silicon. This gives a "boiling point" of GeI_4 of 617°K, and from Eq. (B-2), a force constant ϵ/k of 750°K.

The calculated diffusion coefficients are shown in Table II, together with the exponent n in T^n characterizing the temperature variation, and the Schmidt number. The kinematic viscosities at 415°C used in estimating the Schmidt number were 0.585 cm^2/sec, 4.84 cm^2/sec or 0.073 cm^2/sec for Ar, He, and I_2 respectively.

Table II Diffusion Coefficient and Schmidt Numbers at 415°C

Binary	$\mathcal{D}$ cm^2/sec	Temperature Variation (n in T^n)	N_{Sc}
$Ar-I_2$	0.34	1.81	1.7 (dilute I_2 in Ar)
$He-I_2$	1.61	1.67	3.0 (dilute I_2 in He)
GeI_4-I_2	0.057	2.00	1.3 (dilute GeI_4 in I_2)
$Ar-GeI_4$	0.22	1.54	-
$He-GeI_4$	1.09	1.64	-

APPENDIX C. Toor's Method

The transfer rate for a ternary mixture is given by Eq. (33) of Ref. 10. With the mass average velocity as the reference velocity, the flux is also in mass units (i.e., the left hand side of Eq. (33) of Ref. 10 is n_{io}) and the concentration units on the right hand side are mass per unit volume (equal to $C\,M_i x_i$ for an ideal gas). For the rotating disk system, the mass transfer coefficients in Eq. (33) of Ref. 10 are proportional to the square root of appropriate diffusion coefficients. Aside from a constant factor, the form of Eq. (33) of Ref. 10 applicable to the system under consideration is:

$$n_{io} \propto M_i \sqrt{D_i^m}\,\Delta x_i + \left[\frac{\sqrt{D_i^m}-\sqrt{D_j^m}}{D_i^m - D_j^m}\right]\left[M_i\left(D_{ii}^m - D_i^m\right)\Delta x_i + M_j D_{ij}^m \Delta x_j\right] \quad \text{(C-1)}$$

The driving forces are: $\Delta x_1 = -x_{1\infty}$ and $\Delta x_2 = x_{20}$. When Eq. (C-1) is written for i = 1 and i = 2 and the ratio n_{10}/n_{20} given by Eq. (37), the following relation for the determination of the unknown x_{20} results:

$$\sqrt{D_1^m} + \left[\frac{\sqrt{D_1^m}-\sqrt{D_2^m}}{D_1^m - D_2^m}\right]\left[\left(D_{11}^m - D_1^m\right) - \frac{M_2}{M_1} D_{12}^m \frac{x_{20}}{x_{1\infty}}\right] =$$

$$2\sqrt{D_2^m}\,\frac{x_{20}}{x_{1\infty}} + 2\left[\frac{\sqrt{D_1^m}-\sqrt{D_2^m}}{D_1^m - D_2^m}\right]\left[\left(D_{22}^m - D_2^m\right)\frac{x_{20}}{x_{1\infty}} - \frac{M_1}{M_2} D_{21}^m\right] \quad \text{(C-2)}$$

The D_{ij}^m required in the above relation can be obtained by comparing the defining equation (Eq. (2) of Ref. 10) with Eqs. (6) and (7) of this paper (the first term on the right of Eq. (2) of Ref. 10 is equal to the $\underline{j}_i$ in Eq. (6) of this paper). This yields:

$$D_{11}^{m} = \frac{\mathcal{D}_{13}}{\bar{M}\,\bar{\mathcal{D}}}\left[x_1\ \mathcal{D}_{23}\ M_3 + x_2\ \mathcal{D}_{12}\ M_2 + x_3\ \mathcal{D}_{12}\ M_3\right] \qquad \text{(C-3)}$$

and

$$D_{12}^{m} = \frac{\mathcal{D}_{13}}{\bar{M}\,\bar{\mathcal{D}}}\ \frac{M_1}{M_2}\ x_1\left(\mathcal{D}_{13}M_3 - \mathcal{D}_{12}M_2\right) \qquad \text{(C-4)}$$

$\bar{M}$ and $\bar{\mathcal{D}}$ are given by Eqs. (9) and (7f). Expression for D_{22}^{m} and D_{21}^{m} can be obtained by interchanging the subscripts 1 and 2 in Eqs. (C-3) and (C-4). The same practical diffusion coefficients result if Eqs. (26) of Ref. 10 (which are based on a molar average reference velocity) are converted to D_{ij}^{m} by the methods presented in Ref. 11. The coefficients D_1^m and D_2^m are obtained from Eq. (21) of Ref. 10 with the larger D_i^m associated with the larger D_{ii}^{m}. Following Toor, the concentrations in Eqs. (C-3) and (C-4) were taken as the average of the terminal mole fractions (i.e. $x_1 = 1/2\ x_{1\infty}$ and $x_2 = 1/2\ x_{20}$ for this case).

For a given value of $x_{1\infty}$, the unknown x_{20} is obtained by solution of Eq. (C-2). A trial value of x_{20} is chosen and the required 6 diffusion coefficients computed. The left hand and right hand side of Eq. (C-2) are then calculated. If these two are equal, the trial x_{20} is correct; if not, a new x_{20} is chosen and the process repeated.

Once x_{20} has been obtained, $\Gamma(x_{1\infty})$ of Eq. (52) can be obtained. The denominator of Eq. (52) can be obtained from Eq. (C-1) by letting x_1 and x_2 go to zero. This yields

$$\left(\frac{n_{10}}{x_{1\infty}}\right)_{x_{1\infty}\to 0} \alpha - \sqrt{D_{13}}\ M_1 \qquad \text{(C-5)}$$

The numerator of Eq. (52) is obtained by dividing Eq. (C-1) by $x_{1\infty}$. The result is

$$\Gamma(x_{1\infty})_{\text{Toor}} = \frac{\text{LHS of Eq. (C-2)}}{\sqrt{D_{13}}} \qquad \text{(C-6)}$$

FIGURE CAPTIONS

Fig. 1 Exact and approximate axial velocity profiles on a rotating disk.

Fig. 2 Variation of rate with disk speed - 415°C, iodine inlet mole fraction of 0.126.

Fig. 3 Effect of interfacial velocity parameter B on rate.

Fig. 4 Comparison of experimental and theoretical Γ values - 415°C, 900 RPM, variable iodine inlet mole fraction.

Fig. 5 Density profiles for $N_{Sc} = 1$, $\rho_o/\rho_\infty = 2$ according to Eqs. (A-7), (A-9), and (A-10).

Fig. 6 Functions required for momentum integral computation of density variation effect on rotating disk flow.

Fig. 7 Axial velocity profiles obtained by the momentum integral method for $\beta = 0$ and $\beta = 1.287$, $\Phi = 0.42$.

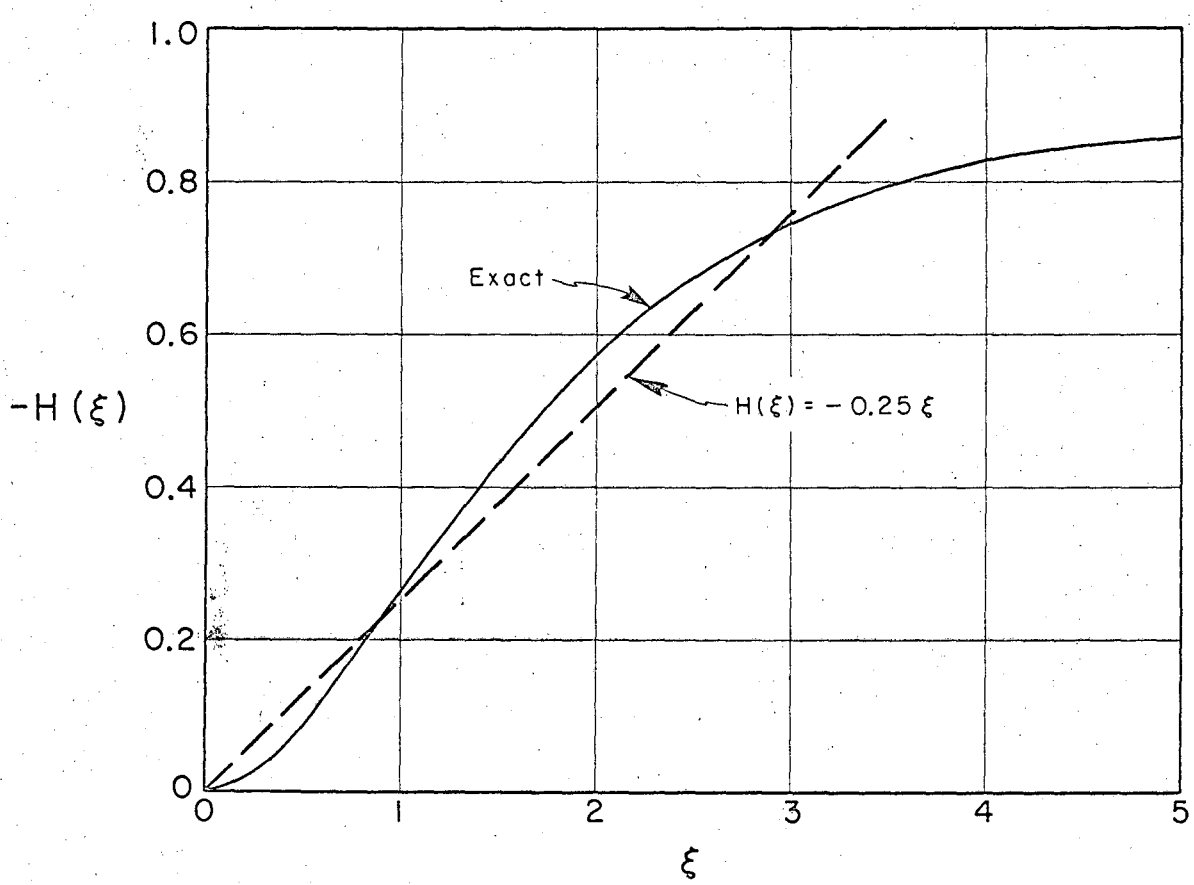

MUB-7706-A

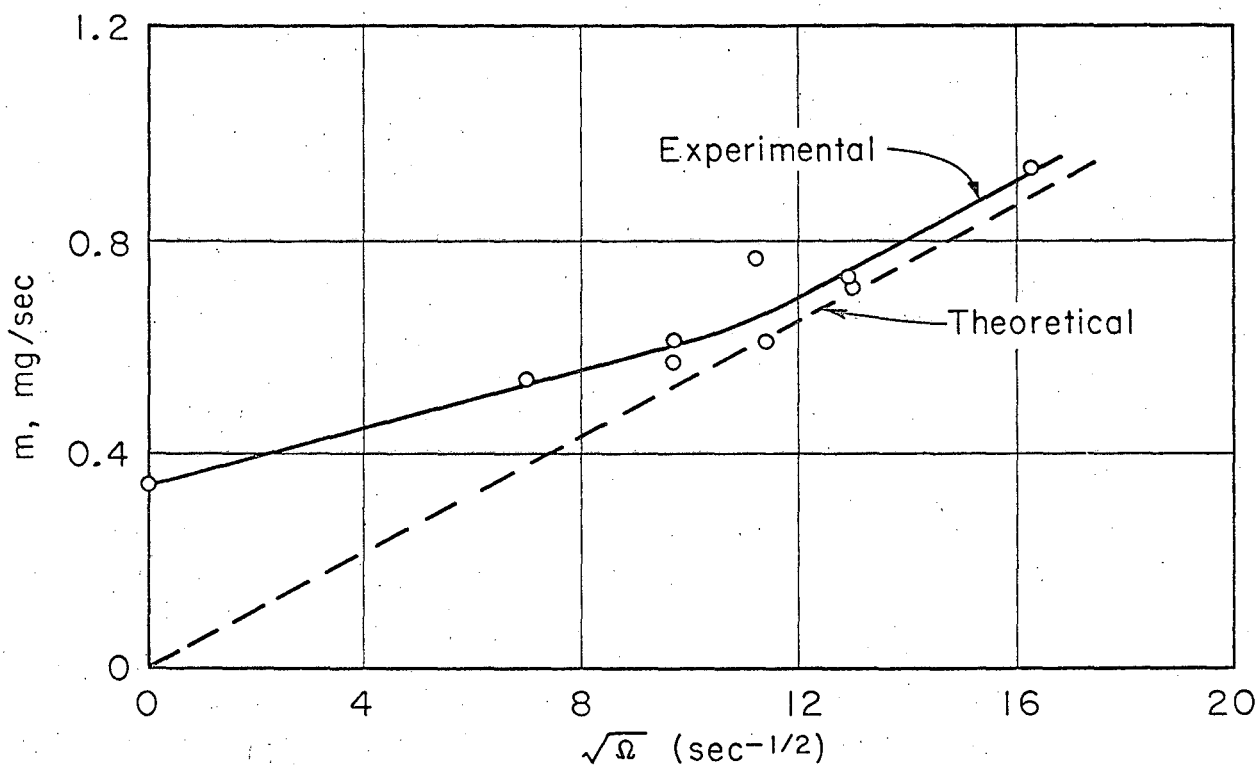
1.2
0.8
0.4
0
m, mg/sec
Experimental
Theoretical
0
4
8
12
16
20
$\sqrt{\Omega}$ (sec$^{-1/2}$)

MUB-7403

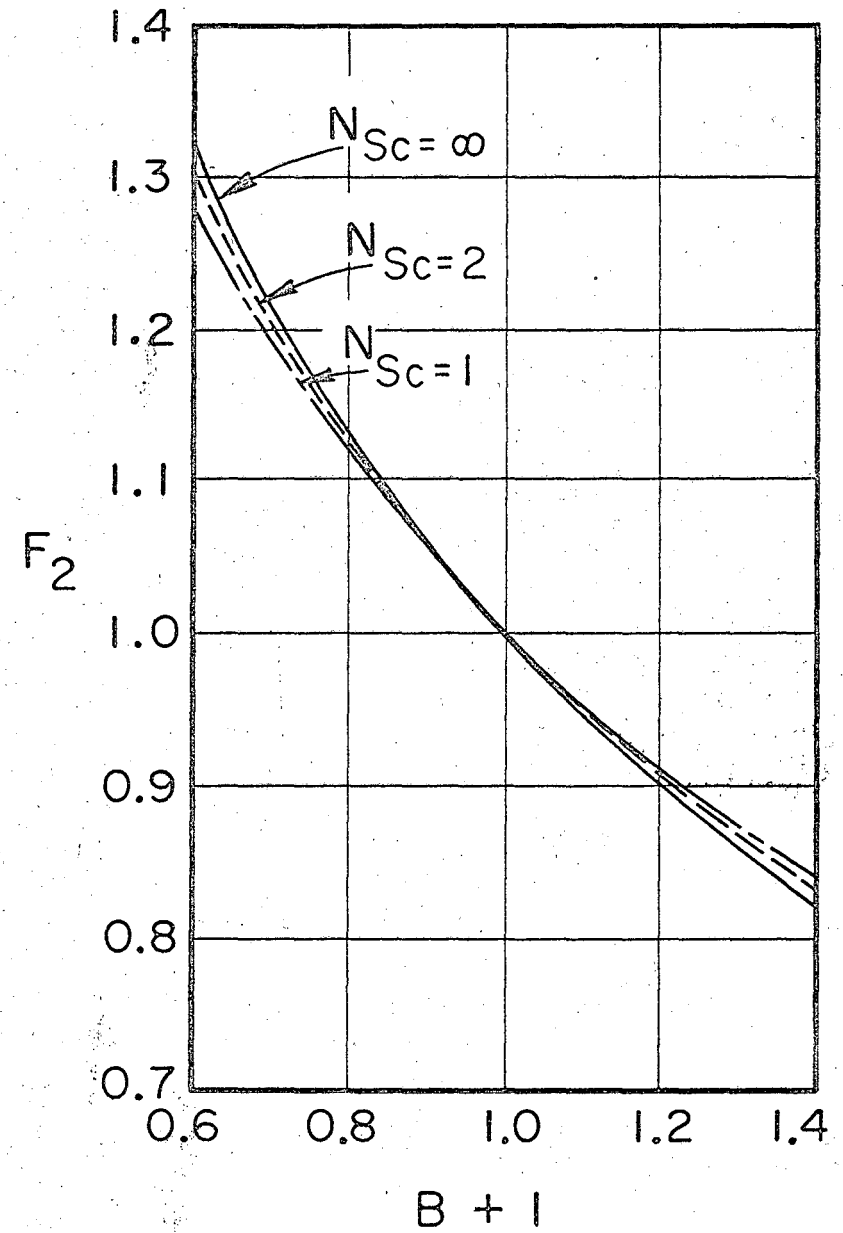

MUB-7707

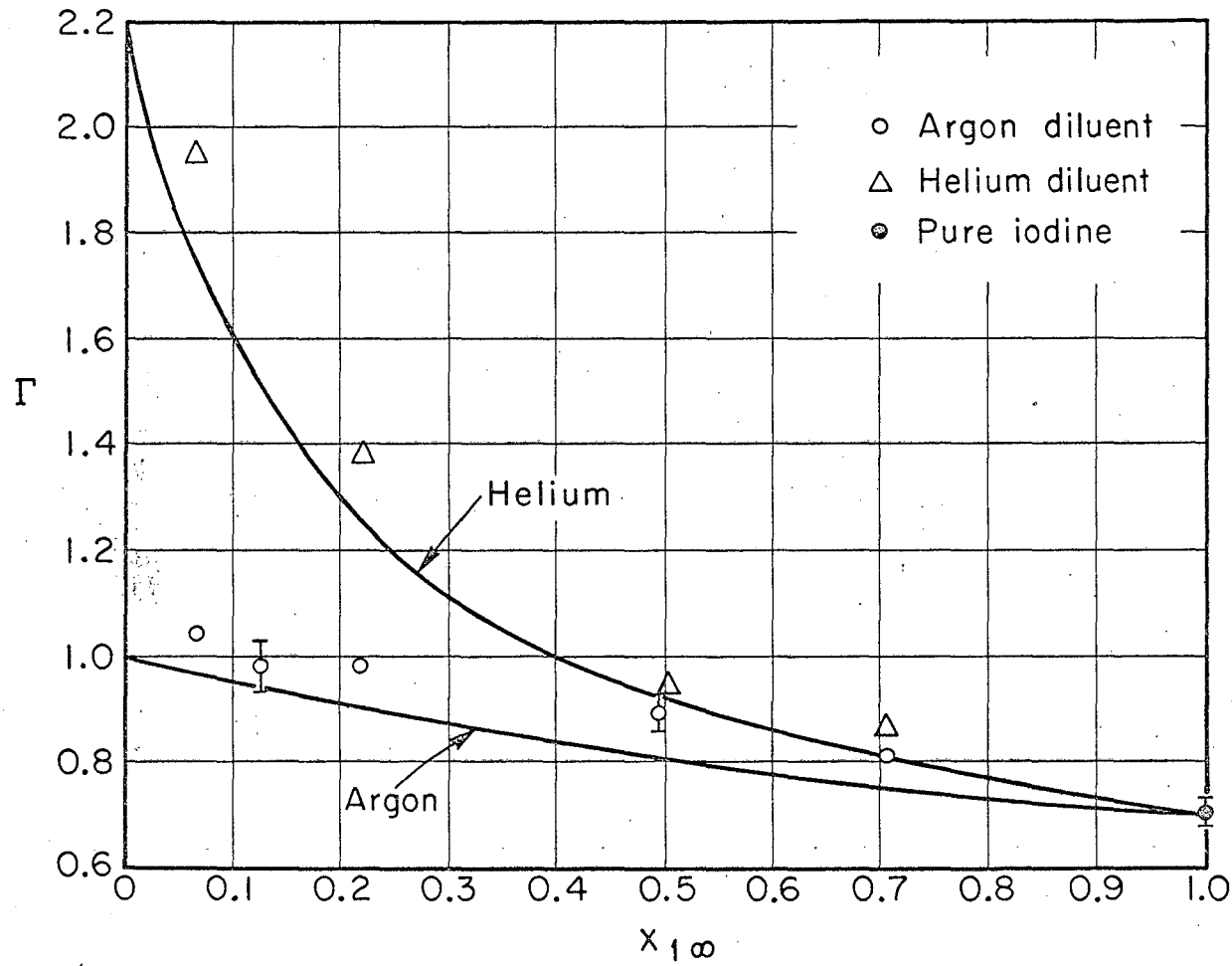
2.2
2.0
1.8
1.6
1.4
1.2
1.0
0.8
0.6
Γ
0
0.1
0.2
0.3
0.4
0.5
0.6
0.7
0.8
0.9
1.0
$X_{1\infty}$
Argon diluent
Helium diluent
Pure iodine
Helium
Argon

MUB-7703

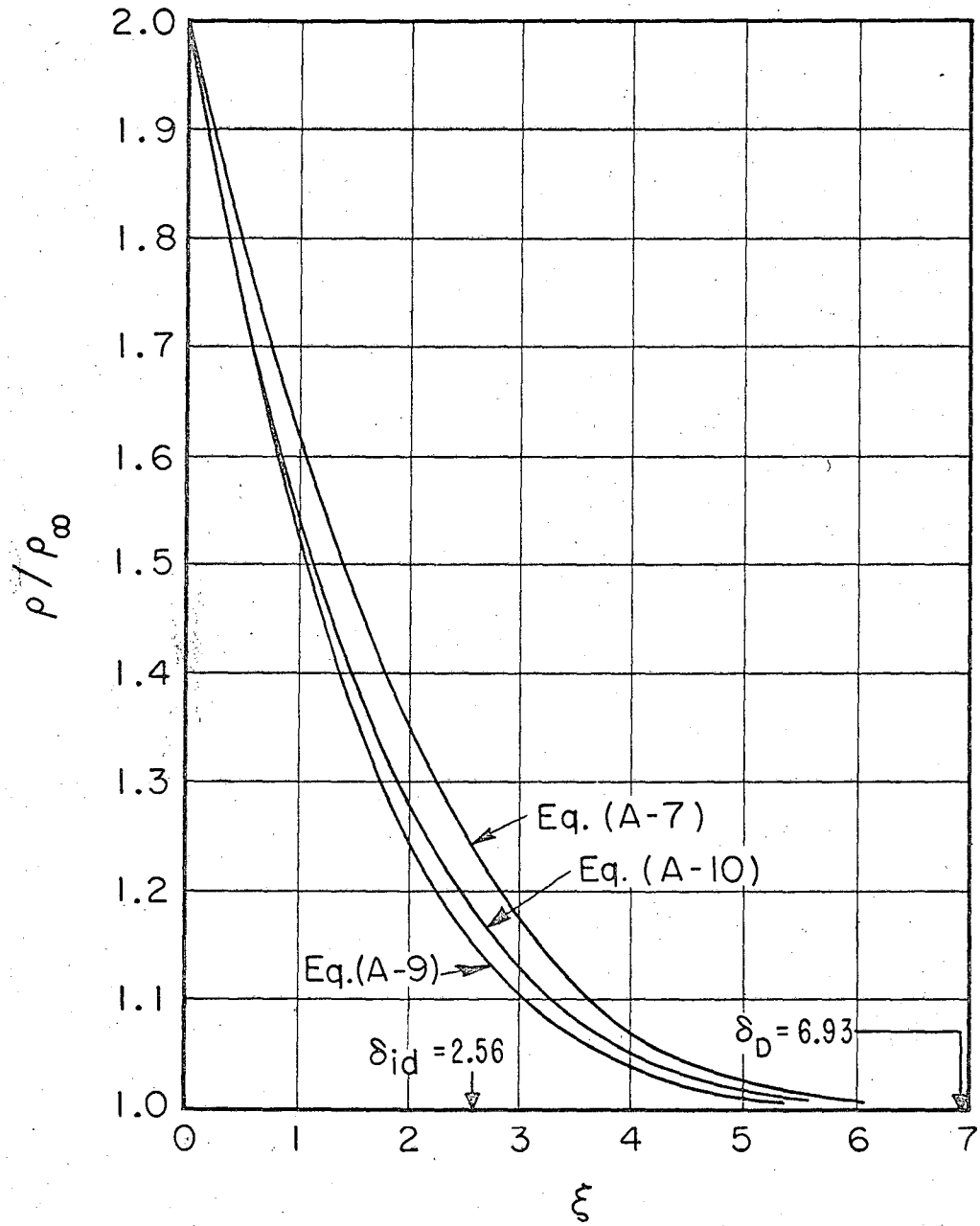
2.0
1.9
1.8
1.7
1.6
1.5
1.4
1.3
1.2
1.1
1.0
ρ/ρ_∞
0
1
2
3
4
5
6
7
ξ
Eq. (A-7)
Eq. (A-10)
Eq.(A-9)
δ_{id} = 2.56
δ_D = 6.93

MUB-7705

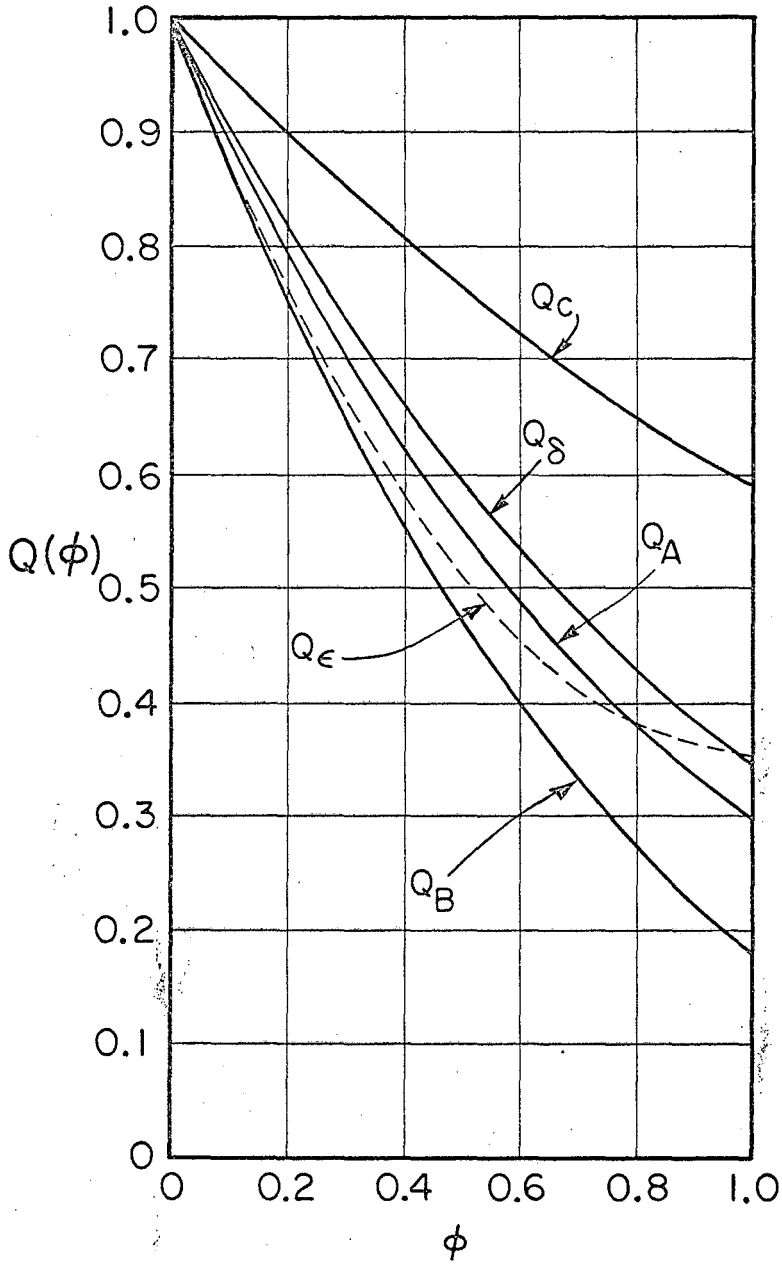
1.0
0.9
0.8
0.7
0.6
0.5
0.4
0.3
0.2
0.1
0
Q(φ)
0
0.2
0.4
0.6
0.8
1.0
φ
Q_C
Q_δ
Q_A
Q_ϵ
Q_B

MUB-7708

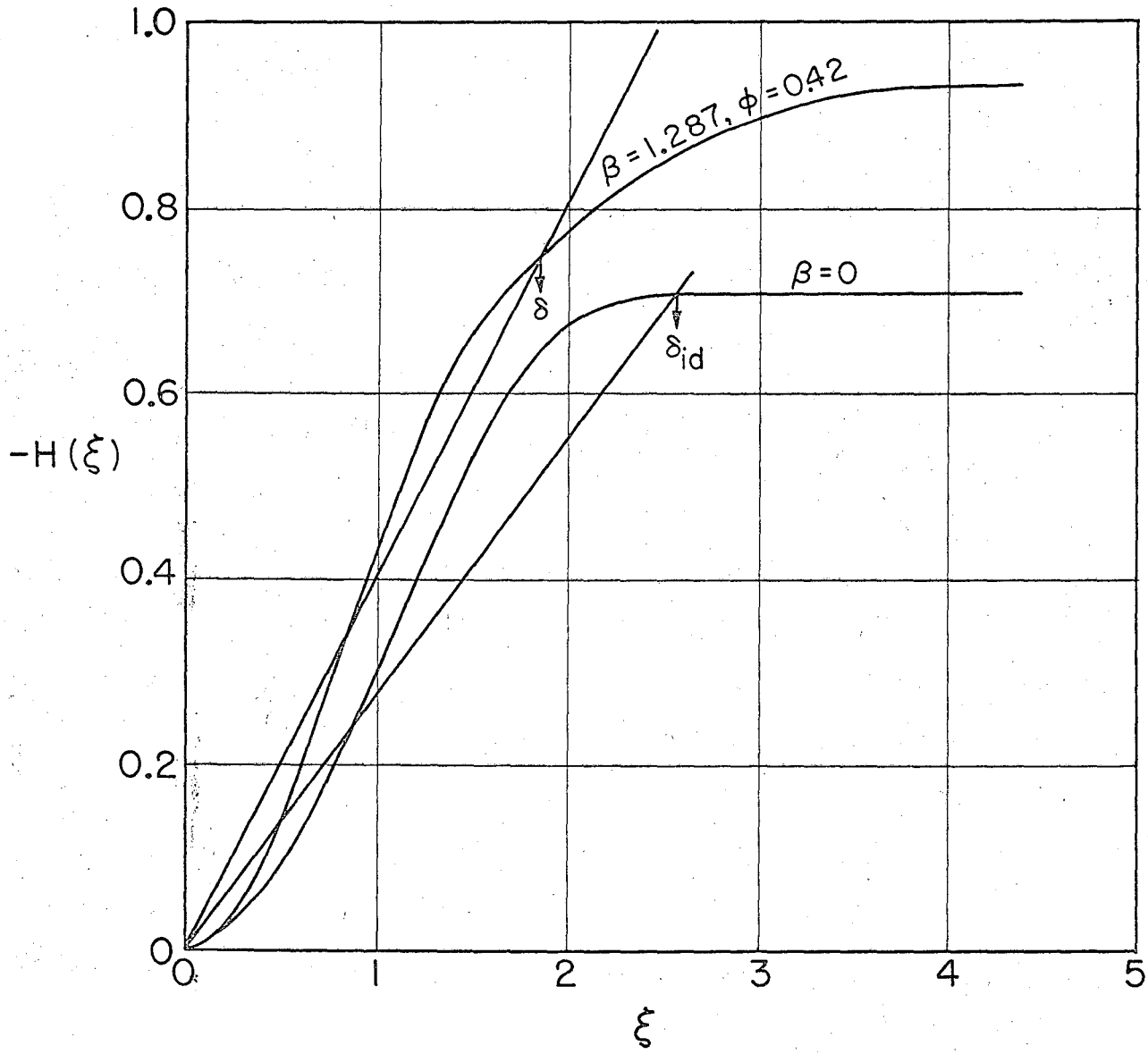
1.0
0.8
0.6
0.4
0.2
0
0
1
2
3
4
5
$-H(\xi)$
ξ
$\beta = 1.287, \phi = 0.42$
$\beta = 0$
δ
δ_{id}

MUB-9305

This report was prepared as an account of Government sponsored work. Neither the United States, nor the Commission, nor any person acting on behalf of the Commission:

A. Makes any warranty or representation, expressed or implied, with respect to the accuracy, completeness, or usefulness of the information contained in this report, or that the use of any information, apparatus, method, or process disclosed in this report may not infringe privately owned rights; or

B. Assumes any liabilities with respect to the use of, or for damages resulting from the use of any information, apparatus, method, or process disclosed in this report.

As used in the above, "person acting on behalf of the Commission" includes any employee or contractor of the Commission, or employee of such contractor, to the extent that such employee or contractor of the Commission, or employee of such contractor prepares, disseminates, or provides access to, any information pursuant to his employment or contract with the Commission, or his employment with such contractor.